Astron. Astrophys. 338, 563–575 (1998)

ASTRONOMY AND ASTROPHYSICS

An analysis of DA white dwarfs from the Hamburg Quasar Survey⋆

D. Homeier[1], **D. Koester**[1], **H.-J. Hagen**[2], **S. Jordan**[1], **U. Heber**[3], **D. Engels**[2], **D. Reimers**[2], **and S. Dreizler**[4]

[1] Institut für Theoretische Physik und Astrophysik der Christian-Albrechts-Universität, Leibnizstraße 15, D-24098 Kiel, Germany (homeier,koester,jordan@astrophysik.uni-kiel.de)
[2] Hamburger Sternwarte, Gojenbergsweg 112, D-21029 Hamburg, Germany (hhagen,dengels,dreimers@hs.uni-hamburg.de)
[3] Dr.-Remeis-Sternwarte Bamberg, Universität Erlangen-Nürnberg, Sternwartstraße 7, D-96049 Bamberg, Germany (heber@sternwarte.uni-erlangen.de)
[4] Institut für Astronomie und Astrophysik, Waldhäuser Straße 64, D-72076 Tübingen, Germany (dreizler@astro.uni-tuebingen.de)

Received 30 March 1998 / Accepted 22 June 1998

Abstract. Follow-up spectroscopy of several hundred hot stars detected by the Hamburg Quasar Survey (HQS) has been carried out between 1989 and 1996. We present the analysis of 80 DA white dwarfs using model atmospheres and theoretical cooling tracks to derive the atmospheric parameters $T_{\rm eff}$ and $\log g$, masses and absolute magnitudes. The HQS turned out to be sensitive to the detection of hydrogen-rich white dwarfs in a wide temperature range, from 10 000 K upwards. Star counts within four HQS fields for magnitudes $B \leq 16\overset{\rm m}{.}4$ exceed those from the Palomar Green survey by about 50%. The more recent observation campaigns emphasized the detection of very hot degenerates, yielding a large fraction of DA stars with $T_{\rm eff} >$ 50 000 K compared to other surveys. The mean mass of our DA sample is M=0.61$\rm M_\odot$, with three massive DA stars exceeding $1\rm M_\odot$ and three DA stars with masses significantly below the assummed lower mass limit for single white dwarf evolution of $0.45\rm M_\odot$. Among the cool DA stars, thirteen are potential ZZ Ceti candidates because their effective temperatures lie close to the instability strip.

Key words: white dwarfs – stars: statistics – surveys

1. Introduction

The Hamburg Schmidt Survey for bright quasars in the northern hemisphere (Hagen et al. 1995) has produced a large database of objective prism spectra for both extragalactic and stellar objects at higher galactic latitudes. It is thus a rich source for subluminous stars, in particular hot subdwarfs and white dwarfs. From the results of the Palomar-Green (PG) Survey (Green et al. 1986, GSL hereafter) a cumulative surface density of 0.19 DA white dwarfs and 0.19 sdO/sdB subdwarfs per square degree can be predicted at the limiting magnitude of the HQS of $B = 17\overset{\rm m}{.}5$. In the PG Survey, which is essentially limited to $B \leq 16\overset{\rm m}{.}2$ and has a color cut-off of $U - B < -0\overset{\rm m}{.}4$, sdB stars form the predominant population.

A collaboration between the Hamburg observatory and the institutes in Kiel and Bamberg has been established to explore this stellar content and has so far carried out follow-up spectroscopy of 285 stars selected from the survey. These observations have led to the independent discovery of 69 DA white dwarfs, 32 white dwarfs of other types, and a large number of early-type subdwarfs. Additional hot stars, 11 DA among them, have been discovered in the follow-up spectroscopy of quasar candidates.

Results for several particularly interesting objects have been published during the recent years: The binary system PG 0824+289 consisting of a DA white dwarf and a carbon dwarf, which was misclassified in the PG survey (Heber et al. 1993); the DAB star HS 0209+0832 with variable helium line profiles in the "DB gap" between about 28 000 and 45 000 K, where no other objects with detectable amounts of helium have been discovered so far (Jordan et al. 1993, Heber et al. 1997); six hot white dwarfs exhibiting metal absorption lines from ultra-highly excited ionization stages probably due to mass-loss from a hot and fast wind (Dreizler et al. 1995, Werner et al. 1995); HS 0704+6153, a PG 1159 star with a relatively low effective temperature of 75 000 K (Dreizler et al. 1994a, Dreizler & Heber 1998); HS 2324+3944, which is unique among a group of only four PG 1159 stars exhibiting hydrogen in the atmosphere since it undergoes pulsations, (Dreizler et al. 1996) and several new hot helium-rich white dwarfs (Dreizler & Werner 1996). Two double DA degenerates, one of them with a component in the ZZ Ceti instability strip are described in Jordan et al. (1998). A summary of the helium-rich subluminous stars is given by Heber et al. (1996) and a brief description of the analysis of 47 sdO stars from the HS survey can be found in Lemke et al. (1998).

The DA white dwarfs form a major fraction of the remaining hot stars, and a detailed analysis will not only enlarge the database of white dwarfs with spectroscopically determined pa-

Send offprint requests to: D. Homeier

⋆ Based on observations collected at the German-Spanish Astronomical Center (DSAZ), Calar Alto, operated by the Max-Plank-Institut für Astronomie Heidelberg jointly with the Spanish National Commission for Astronomy; with the International Ultraviolet Explorer satellite (IUE) collected at Villafranca, Spain, and with the ROSAT X-ray telescope.

rameters, but yields also important information about the temperature and mass distribution of the stellar content of this survey. Accurate effective temperatures are essential for the construction of the white dwarf luminosity function. From the fundamental stellar parameters masses and luminosities can be derived using theoretical cooling models, thus providing information about the mass distribution and the spatial distribution of white dwarfs. The large coverage of the survey proves especially advantageous for the investigation of relatively rare subtypes, such as the ZZ Ceti variables or the very hot DA. The number of known DA hotter than 50 000 K is increased by 25% by this survey, which will improve the statistics at the bright end of the white dwarf luminosity function. A better sampling of this part of the LF constrains the cooling models for hot white dwarfs which involve neutrino emission as primary means of heat loss. These relatively luminous white dwarfs, in combination with the low magnitude limit of the survey, can also probe more effectively the galactic scale height of the white dwarf population. Both scale height and luminosity function provide information about the structure and age as well as the star formation history of the Galactic disk.

Fitting of the Balmer line profiles to theoretical spectra has now been firmly established as the most accurate method for determining the fundamental stellar parameters (Finley et al. 1997, FKB hereafter). We present here the results of an analysis of all follow-up spectra using the latest LTE model atmospheres.

2. The Hamburg Quasar Survey

The objective prism plates for the survey are taken with the 80 cm Hamburg Schmidt Reflector, operating at the *Deutsch-Spanisches Astronomiezentrum* (DSAZ) on Calar Alto, Spain since 1980. A $1.^\circ 7$ prism is used, providing spectra with reciprocal dispersion of 1390 Å/mm at Hγ on $24 \times 24\ \mathrm{cm}^2$ plates, corresponding to a field size of $5.^\circ 5 \times 5.^\circ 5$. Under good seeing conditions the FWHM of the images reaches the plate resolution of 30 μm, which translates to a spectral resolution of 45 Å at Hγ. Additional unfiltered direct plates for each field are serving for position measurement and recognition of spectral overlaps.

Both objective prism and direct images are taken on hypersensitized KODAK IIIa-J plates, recording spectra between $\lambda \approx 3400$Å and $\lambda \approx 5400$Å within a usable magnitude range of $13.^{\mathrm{m}}5 \leq B \leq 18.^{\mathrm{m}}5$. The full survey area is now covered by two prism plates for each of the 567 fields. (Engels et al. 1998).

The uncalibrated plates are digitized in Hamburg with a PDS-microdensitometer. Digitized scans for all 30 – 50 000 spectra on each plate are available in a low resolution mode (LRS). High resolution scans (HRS) at full plate resolution exist for 1 000–3 000 objects per plate extracted with the help of an automated search software selecting for blue continua. Blue objects were found to be complete within the HRS data base down to $B \approx 17.^{\mathrm{m}}5$ (Hagen et al. 1995).

These scans can be evaluated interactively and are classified into a number of stellar and non-stellar categories. The strong Balmer lines of DA white dwarfs, in particular, are among the features that can be easily identified even at this resolution (white dwarfs brighter $\approx 16.^{\mathrm{m}}5$ and cooler than 20 000 K clearly show broad absorption lines on the fine scans). On the prism plates, brightness calibration of the spectra is performed in the range of the Johnson B filter. With the help of photometric sequences B magnitudes for all objects are determined which are accurate to better than $0.^{\mathrm{m}}5$.

The selection criteria developed by the Hamburg group are designed to efficiently extract UV-excess sources from the LRS database, and comparisons with samples of known blue stars have shown that white dwarfs down to at least $T_{\mathrm{eff}} \approx 10\,000$ K and hot subdwarfs are recovered in the High Resolution Scans.

Table 1. Observation log of the follow-up spectroscopy programme

Date	Instrument	rec. disp. Å/mm	Wavelength range Å	observers
Jan 89	3.5m Cass	240	3400–6750	Hagen & Reimers
Jan 89	3.5m B&C	120	3850–5650	Heber & Jordan
Jan 89	2.2m Cass	288	3790–7170	Hagen
Jan 90	3.5m Twin	144/160	3550–5550, 5570–7030	Jordan & Möller
Okt 90	3.5m FR	134	3770–5550	Heber & Dreizler
Nov 90	3.5m Twin	144/160	3430–5550, 5560–7030	Jordan & Rauch
Jun 91	3.5m Twin	144/160	3570–5750, 5110–9300	Heber & Marten
Aug 92	3.6m EFOSC	200	3750–6880	Bade
Sep 92	3.5m Twin	144/160	3360–5550, 5430–9740	Dreizler
Mar 93	3.5m Twin	144/160	3470–5680, 5420–9630	Heber
Mar 93	2.2m Cass	240	3300–8500	Hagen
Sep 93	3.5m Twin	72/72	3600–5500, 5540–7420	Dreizler & Haas
	2.2m B&C	120	4010–6720	Haas & Dreizler
Apr 94	2.2m Cass	900	3250–8200	Hagen
Sep 94	3.5m Twin	72/72	3610–5490, 5440–7320	Dreizler
Jan 95	3.5m Twin	72/72	3580–5470, 5420–7320	Dreizler
Jun 96	3.5m Twin	72/72	3610–5510, 5440–7320	Dreizler
Aug 96	3.5m Twin	72/72	3770–5660, 5430–7340	Lemke
Oct 96	2.2m CAFOS	400	3400–9200	Hagen

3. The hot star programme

3.1. Follow-up observations

Motivations and first results of the hot star survey, which started in 1989, have been first described in Heber et al. (1991), Jordan et al. (1991) and Jordan & Heber (1993). A more comprehensive description of results was later given by Dreizler et al. (1994b).

For the pilot project the very deep and well-studied HQS field +47.5/22 was chosen, supplemented by the fields +47.5/28, +62.5/25 and +77.5/15 (the fields are denoted by the declination of the plate center and numbered by right ascension). Until 1996 candidates from 33 additional fields were included in the observations.

After white dwarf and subdwarf candidates had been selected by automatic and visual inspection of the objective prism scans, follow-up spectroscopy was performed during eleven observing runs at the DSAZ (see Table 1). The data from early observing runs were reduced using the IDAS package written by G. Jonas in Kiel as described in Groote et al. (1989), while data obtain from 1991 onwards were reduced using the MIDAS package. A relative flux calibration was attempted using the standard stars G191-B2B, Feige 34 and BD+28°4211. Due to variable weather conditions and the chosen slit width (2 $''$), however, the flux calibration is not always reliable.

Table 2. Distribution of the 300 objects observed in the hot star programme

Types	No.	Types	No.
DA	69	PG 1159	4
DAB/DAO	7	sdO	59
DA+M, DAe	4	sdB	93
DB	3	HBA/HBB	27
DO	9	sdF	13
mag. WD	1	other	11

Over the years the discrimination between the QSO candidates and blue stellar candidates has become very efficient. Moreover, the classification among the blue stars is also very reliable now; during the first two observation run we still had many horizontal branch A and B stars as well as population II sdF and sdG stars in our sample. On field +47.5/22, for example, 31 observations were necessary to find 9 DAs and 3 sdB stars among 9 sdF and 10 HB stars; in the 1991 campaign on +62.5/25 we already had a sample of 6 DAs and 7 sdBs with only a single sdF.

During the more recent observation runs the aim of our follow-up spectroscopy was shifted towards the discovery of particularly hot white dwarfs, subdwarfs, and PG1159 stars. Thus we covered a larger sky area while excluding those stars that could be easily identified as cool DA on the objective-prism plates. In the future we plan to publish a list of WD identifications based on the HRS spectra alone (Homeier et al. in prep.). In this paper we present the results of the analysis of the sample of DA white dwarfs for which follow-up spectroscopy has been performed.

The total number of stars in the original hot star programme is 300, 152 of which have been classified as early-type subdwarfs, 97 as degenerates and 51 as other stars of various types, mainly horizontal branch stars of A and B-type and later-type subdwarfs. (cf. Table 2). In addition to these stellar objects two quasars have been observed. An additional number of 11 DA white dwarfs has been discovered in the follow-up spectroscopy of quasar candidates by the Hamburg group at the DSAZ (observations by Hagen) and at ESO (Bade). With the exception of HS 0138+0451, which could only be visually classified DA2.5 from a printed spectrum, these stars have also been included in our analysis.

The overall number ratios between the different object classes are similar to those found in the PG survey for a limiting magnitude of B = 16.$^{\rm m}$0–16.$^{\rm m}$4 (Fig. 2 in GSL) rather than those expected for a deeper sample. Since the sample for all fields is far from being complete down to the limiting magnitude, we will not attempt any statistical analysis here.

In all cases we have checked for overlap with other surveys using SIMBAD. Stars discovered in other surveys are listed by alternate names rather than their HS designation in Table 3.1 if a spectroscopic identification as a white dwarf has been found in the literature. HS 0210+1629 (GD 24), HS 0641+6528 (GD 442), HS 1627+7436 (GD 510) were suspected to be white dwarfs from their colours by Giclas et al. (1965, 1970 and 1971). Among the white dwarfs independently discovered in this paper are also PG 1620+648 (HS 1619+6443), whose coordinates are in error in the PG catalog and PG 2235+082, which was misclassified as sdB before. HS 1745+6043 has been reported as a joint ROSAT and *EUVE* detection (EUVE J 1745+607), but not been identified with an optical counterpart (Lampton et al. 1997).

3.2. Star counts and surface densities

Among the stars brighter than B = 16.$^{\rm m}$4 that were discovered by our program, there is a considerable number which have not been found by the Palomar Green survey. Since there is no complete overlap with the circular fields of the PG survey even at latitudes $b > 30°$ and the limiting magnitudes of the fields vary between 15.$^{\rm m}$5 and 16.$^{\rm m}$7, an individual comparison is of little avail. Instead, we will present the surface densities of DA white dwarfs found in our follow-up spectroscopy program, which we found to be in significant disagreement with those reported for the PG survey by GSL.

There are four fields for which comprehensive follow-up spectroscopy has been performed. $+47.5/22$ is the only one of these in which all candidates classified as hot stars according to the selection criteria have been observed. In the other three not all objects selected from the objective prism scans have been spectroscopied yet, so we will regard the number of spectroscopically identified DA white dwarfs as a lower limit to the number of DAs found by the HQS. We chose the subsample of stars brighter than $B = 16.^{\rm m}4$, since this is the deepest magnitude bin for which statistics exist in GSL. We have calculated theoretical colours for all observed DAs as described below and found all of them to satisfy the PG colour criterium of $U - B < -0.^{\rm m}4$.

18 stars in this magnitude range were classified as hot stars within the four fields, 14 of which have been spectroscopically confirmed to be DA white dwarfs. Among these are GD 320, which was identified from the McCook & Sion (1987) catalogue, and a binary DA with an M-dwarf companion which are both not listed in this paper. The cumulative surface density for $B = 16.^{\rm m}4$ given by GSL is $5.4 \cdot 10^{-2}$ DA per square degree, and the logarithmic count slope $d(\log N)/dB = 0.57$ over the range of $14.^{\rm m}4 < B < 16.^{\rm m}4$, consistent with an Euclidean distribution. When galactic scale heights $z \gtrsim 250$ pc are assumed, this slope is expected to continue to $B = 17.^{\rm m}5$, leading to the prediction of 0.19 DA per square degree. For the 120 square degrees of our four HQS fields, 6.5 DA with $B \leq 16.^{\rm m}4$ are to be expected from these figures.

The star counts in GSL are corrected for photometric measuring errors, and we will apply the same correction to our results. The correction to the counts for Gaussian distributed errors in B is given by Eddington (1940) as $-\frac{\sigma_B^2}{2}\frac{d^2N}{dB^2}$, reflecting the systematic diffusion of objects from the more populated fainter magnitude bins into the sample. Since
$\frac{d^2N}{dB^2} = (\ln 10 \cdot \frac{d \log N}{dB})^2 = 1.72$
for the white dwarf count slope of 0.57, with $\sigma_B = 0.^{\rm m}5$ we ob-

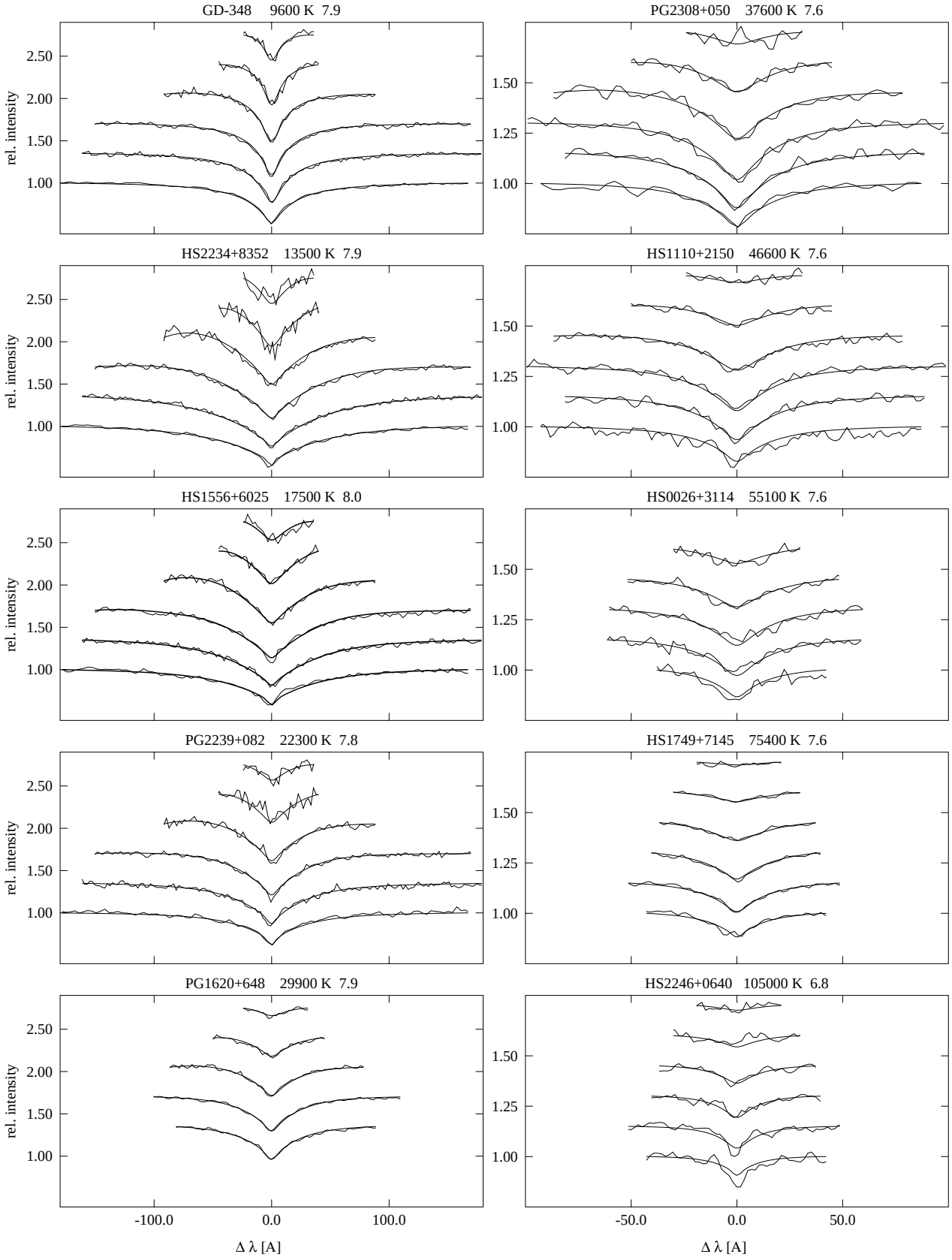

Fig. 1. Sample spectra (observed and theoretical) spanning the full range of effective temperatures. All fitted lines are shown, Hα being normalized to a continuum of 1 and the higher lines offset by equal amounts. Note the different scales in the left and right column

Table 3. Position and observation list of the 80 DA white dwarfs

Name	α_{1950}	δ_{1950}	Field	Date	Instr.	Name	α_{1950}	δ_{1950}	Field	Date	Instr.
HS 0008+3302	$0^{\rm h}08^{\rm m}23^{\rm s}3$	$33\,^\circ02\,'53\,''$	32.5/01	10/96	Cass	GD 348	$15^{\rm h}37^{\rm m}08^{\rm s}1$	$65\,^\circ11\,'31\,''$	62.5/25	06/91	Twin
HS 0009+1621	$0^{\rm h}09^{\rm m}44^{\rm s}6$	$16\,^\circ21\,'38\,''$	17.5/02	10/96	Cass	PG 1541+650	$15^{\rm h}41^{\rm m}08^{\rm s}8$	$65\,^\circ03\,'23\,''$	62.5/25	06/91	Twin
HS 0026+3114	$0^{\rm h}26^{\rm m}02^{\rm s}9$	$31\,^\circ14\,'34\,''$	32.5/02	08/93	Twin	HS 1556+6025	$15^{\rm h}56^{\rm m}03^{\rm s}0$	$60\,^\circ25\,'28\,''$	62.5/25	06/91	Twin
				01/95	Twin	HS 1610+6149	$16^{\rm h}10^{\rm m}54^{\rm s}6$	$61\,^\circ49\,'08\,''$	62.5/25	06/91	Twin
GD 8	$0^{\rm h}37^{\rm m}11^{\rm s}6$	$31\,^\circ16\,'02\,''$	32.5/03	08/93	Twin	HS 1619+6443	$16^{\rm h}19^{\rm m}55^{\rm s}6$	$64\,^\circ43\,'01\,''$	62.5/25	06/91	Twin
HS 0047+0716	$0^{\rm h}47^{\rm m}38^{\rm s}7$	$7\,^\circ16\,'20\,''$	07.5/03	08/92	EFOSC					03/93	Twin
HS 0129+0511	$1^{\rm h}29^{\rm m}37^{\rm s}0$	$5\,^\circ11\,'11\,''$	07.5/06	01/89	B&C					06/96	Twin
HS 0130+0156	$1^{\rm h}30^{\rm m}22^{\rm s}6$	$1\,^\circ56\,'11\,''$	02.5/06	09/93	Cass	HS 1627+7436	$16^{\rm h}27^{\rm m}48^{\rm s}3$	$74\,^\circ36\,'49\,''$	72.5/18	06/91	Twin
HS 0130+0800	$1^{\rm h}30^{\rm m}46^{\rm s}0$	$8\,^\circ00\,'42\,''$	07.5/06	01/89	B&C	HS 1641+7132	$16^{\rm h}41^{\rm m}34^{\rm s}2$	$71\,^\circ32\,'36\,''$	72.5/18	06/91	Twin
HS 0138+0451	$1^{\rm h}38^{\rm m}15^{\rm s}2$	$4\,^\circ51\,'41\,''$	07.5/06	01/88	3.5m Cass	HS 1650+7229	$16^{\rm h}50^{\rm m}03^{\rm s}6$	$72\,^\circ29\,'15\,''$	72.5/18	06/91	Twin
HS 0146+0723	$1^{\rm h}46^{\rm m}54^{\rm s}3$	$7\,^\circ23\,'31\,''$	07.5/06	01/89	Cass	HS 1653+7753	$16^{\rm h}53^{\rm m}17^{\rm s}0$	$77\,^\circ53\,'37\,''$	77.5/15	06/91	Twin
Feige-17	$1^{\rm h}55^{\rm m}03^{\rm s}5$	$6\,^\circ57\,'30\,''$	07.5/07	10/90	FRed	HS 1703+6315 A	$17^{\rm h}03^{\rm m}02^{\rm s}0$	$63\,^\circ15\,'30\,''$	62.5/27	09/93	Cass
HS 0210+1629	$2^{\rm h}10^{\rm m}20^{\rm s}7$	$16\,^\circ29\,'12\,''$	17.5/07	10/90	FRed	HS 1729+7735	$17^{\rm h}29^{\rm m}05^{\rm s}3$	$77\,^\circ35\,'54\,''$	77.5/15	06/91	Twin
HS 0235+0655	$2^{\rm h}35^{\rm m}54^{\rm s}1$	$6\,^\circ55\,'15\,''$	07.5/09	01/89	B&C	HS 1730+7844	$17^{\rm h}30^{\rm m}16^{\rm s}8$	$78\,^\circ44\,'21\,''$	77.5/15	06/91	Twin
HS 0235+0514	$2^{\rm h}35^{\rm m}47^{\rm s}4$	$5\,^\circ14\,'07\,''$	07.5/09	01/89	Cass	HS 1745+6043	$17^{\rm h}45^{\rm m}18^{\rm s}9$	$60\,^\circ43\,'15\,''$	62.5/28	06/91	Twin
GD 41	$3^{\rm h}02^{\rm m}01^{\rm s}2$	$2\,^\circ45\,'21\,''$	02.5/10	09/92	Twin	HS 1749+7145	$17^{\rm h}49^{\rm m}52^{\rm s}9$	$71\,^\circ45\,'56\,''$	72.5/20	08/93	Twin
HS 0348+2803	$3^{\rm h}48^{\rm m}56^{\rm s}4$	$28\,^\circ03\,'09\,''$	27.5/11	10/96	Cass					06/96	Twin (2)
KUV 03520+0500	$3^{\rm h}52^{\rm m}01^{\rm s}3$	$5\,^\circ00\,'00\,''$	02.5/13	06/91	Twin	HS 1817+7852	$18^{\rm h}17^{\rm m}29^{\rm s}6$	$78\,^\circ52\,'52\,''$	77.5/15	09/92	Twin
				10/90	FRed	RE J 1820+580	$18^{\rm h}19^{\rm m}42^{\rm s}8$	$58\,^\circ03\,'13\,''$	57.5/32	09/93	Cass
KUV 03561+0807	$3^{\rm h}56^{\rm m}05^{\rm s}9$	$8\,^\circ07\,'14\,''$	07.5/13	09/93	Twin					08/96	Twin
				09/93	Cass	HS 1822+7452	$18^{\rm h}22^{\rm m}10^{\rm s}0$	$74\,^\circ52\,'28\,''$	77.5/15	06/91	Twin
HS 0401+0001	$4^{\rm h}01^{\rm m}59^{\rm s}3$	$0\,^\circ01\,'43\,''$	02.5/14	01/95	Twin	HS 1827+7753	$18^{\rm h}27^{\rm m}45^{\rm s}3$	$77\,^\circ53\,'39\,''$	77.5/15	06/91	Twin
HS 0421+0342	$4^{\rm h}21^{\rm m}38^{\rm s}4$	$3\,^\circ42\,'00\,''$	02.5/14	03/93	Cass					06/96	Twin (2)
HS 0424+0141	$4^{\rm h}24^{\rm m}16^{\rm s}8$	$1\,^\circ41\,'09\,''$	02.5/14	09/92	Twin	KUV 18453+6819	$18^{\rm h}45^{\rm m}20^{\rm s}6$	$68\,^\circ19\,'18\,''$	67.5/25	06/91	Twin
HS 0503+0154	$5^{\rm h}03^{\rm m}03^{\rm s}3$	$1\,^\circ54\,'28\,''$	02.5/16	01/95	Twin	HS 1917+5954	$19^{\rm h}17^{\rm m}38^{\rm s}9$	$59\,^\circ54\,'20\,''$	57.5/34	06/96	Twin
HS 0507+0434 B	$5^{\rm h}07^{\rm m}34^{\rm s}5$	$4\,^\circ35\,'15\,''$	02.5/16	09/92	Twin	HS 1936+6902	$19^{\rm h}38^{\rm m}24^{\rm s}6$	$69\,^\circ02\,'14\,''$	67.5/25	06/91	Twin
HS 0507+0434 A	$5^{\rm h}07^{\rm m}35^{\rm s}0$	$4\,^\circ34\,'59\,''$	02.5/16	09/92	Twin	HS 2058+0823	$20^{\rm h}58^{\rm m}46^{\rm s}6$	$8\,^\circ23\,'21\,''$	07.5/64	09/92	Twin
HS 0615+6535	$6^{\rm h}15^{\rm m}29^{\rm s}6$	$65\,^\circ35\,'40\,''$	67.5/09	09/92	Twin					06/96	Twin (2)
HS 0641+6528	$6^{\rm h}41^{\rm m}34^{\rm s}1$	$65\,^\circ28\,'50\,''$	67.5/09	11/90	Twin	PG 2120+055	$21^{\rm h}20^{\rm m}05^{\rm s}3$	$5\,^\circ29\,'48\,''$	07.5/65	09/92	Twin
HS 0727+6915	$7^{\rm h}27^{\rm m}34^{\rm s}7$	$69\,^\circ15\,'57\,''$	67.5/11	01/90	Twin	HS 2157+8152	$21^{\rm h}57^{\rm m}18^{\rm s}5$	$81\,^\circ53\,'01\,''$	82.5/13	06/91	Twin
HS 0742+2306	$7^{\rm h}42^{\rm m}33^{\rm s}6$	$23\,^\circ06\,'34\,''$	22.5/22	01/95	Twin	HS 2210+1139	$22^{\rm h}10^{\rm m}58^{\rm s}0$	$11\,^\circ30\,'22\,''$	12.5/67	11/90	Twin
HS 0841+4547	$8^{\rm h}41^{\rm m}32^{\rm s}4$	$45\,^\circ47\,'31\,''$	47.5/20	02/94	Cass	PG 2220+1323	$22^{\rm h}20^{\rm m}46^{\rm s}7$	$13\,^\circ23\,'44\,''$	12.5/67	11/90	Twin
HS 0943+4724	$9^{\rm h}43^{\rm m}45^{\rm s}0$	$47\,^\circ24\,'19\,''$	47.5/22	01/89	B&C	HS 2234+8352	$22^{\rm h}34^{\rm m}36^{\rm s}9$	$83\,^\circ52\,'43\,''$	82.5/13	06/91	Twin
HS 0943+4852	$9^{\rm h}43^{\rm m}55^{\rm s}3$	$48\,^\circ52\,'14\,''$	47.5/22	01/89	Cass	PG 2235+082	$22^{\rm h}35^{\rm m}05^{\rm s}3$	$8\,^\circ13\,'14\,''$	07.5/69	11/90	Twin
HS 0946+4848	$9^{\rm h}46^{\rm m}20^{\rm s}3$	$48\,^\circ48\,'06\,''$	47.5/22	01/89	Cass	HS 2236+3118	$22^{\rm h}36^{\rm m}03^{\rm s}5$	$31\,^\circ18\,'41\,''$	32.5/59	08/93	Twin
HS 0946+5009	$9^{\rm h}46^{\rm m}48^{\rm s}1$	$50\,^\circ09\,'50\,''$	47.5/22	01/89	B&C	PG 2239+082	$22^{\rm h}39^{\rm m}12^{\rm s}9$	$8\,^\circ09\,'30\,''$	07.5/69	06/91	Twin
HS 0949+4935	$9^{\rm h}49^{\rm m}31^{\rm s}7$	$49\,^\circ35\,'01\,''$	47.5/22	01/89	B&C	HS 2240+1234 B	$22^{\rm h}40^{\rm m}01^{\rm s}7$	$12\,^\circ34\,'20\,''$	12.5/68	10/90	FRed
HS 0951+3620	$9^{\rm h}51^{\rm m}38^{\rm s}3$	$36\,^\circ20\,'30\,''$	37.5/25	01/95	Twin	HS 2240+1234 A	$22^{\rm h}40^{\rm m}02^{\rm s}5$	$12\,^\circ34\,'23\,''$	12.5/68	10/90	FRed
HS 1001+4651	$10^{\rm h}01^{\rm m}25^{\rm s}5$	$46\,^\circ50\,'59\,''$	47.5/22	01/90	Twin	HS 2244+0305	$22^{\rm h}44^{\rm m}49^{\rm s}7$	$3\,^\circ05\,'57\,''$	02.5/69	09/92	Twin
HS 1002+4518	$10^{\rm h}02^{\rm m}59^{\rm s}0$	$45\,^\circ18\,'42\,''$	47.5/22	01/90	Twin	HS 2246+0640	$22^{\rm h}46^{\rm m}54^{\rm s}0$	$6\,^\circ40\,'53\,''$	07.5/69	06/91	Twin
HS 1003+4852	$10^{\rm h}03^{\rm m}47^{\rm s}9$	$48\,^\circ52\,'36\,''$	47.5/22	01/90	Twin					06/96	Twin (2)
HS 1110+2150	$11^{\rm h}10^{\rm m}26^{\rm s}3$	$21\,^\circ50\,'40\,''$	22.5/32	01/95	Twin	PG 2308+050	$23^{\rm h}08^{\rm m}45^{\rm s}4$	$5\,^\circ03\,'12\,''$	07.5/71	09/92	Twin
Ton-82	$12^{\rm h}31^{\rm m}02^{\rm s}7$	$46\,^\circ29\,'58\,''$	47.5/28	01/89	B&C	HS 2330+0556	$23^{\rm h}30^{\rm m}32^{\rm s}5$	$5\,^\circ56\,'37\,''$	07.5/72	10/90	FRed
GD 148	$12^{\rm h}32^{\rm m}33^{\rm s}1$	$47\,^\circ54\,'06\,''$	47.5/28	01/89	B&C	PG 2353+027	$23^{\rm h}53^{\rm m}53^{\rm s}8$	$2\,^\circ40\,'24\,''$	02.5/01	09/92	Twin
PG 1234+482	$12^{\rm h}34^{\rm m}23^{\rm s}4$	$48\,^\circ11\,'57\,''$	47.5/28	01/89	B&C					06/96	Twin (2)
HS 1241+4821	$12^{\rm h}41^{\rm m}22^{\rm s}0$	$48\,^\circ21\,'58\,''$	47.5/28	01/89	B&C						

tain a correction of -21.5% to the counts, reducing our number to 11 DAs. This is still barely within 2σ of the predicted 6.5.

We hope to review this discrepancy on the basis of a larger sample and with better photometry. Engels et al. (1994) have shown that the accuracy of the magnitudes determined from the objective prism plates can be improved to $0\overset{\rm m}{.}15$ with suitable photometric sequences.

4. Analysis of the optical spectra

4.1. Models

The spectroscopic techniques to determine effective temperatures and surface gravities from a model fit to the Balmer line profile have been first applied to a large sample of white dwarfs by Bergeron et al. (1992, BSL hereafter). More recent studies of both optically and EUV-selected samples have been published by FKB, Marsh et al. (1997) and Vennes et al. (1997).

The observed spectra have been fitted to an extensive grid of models for pure hydrogen atmospheres covering the range from 6 000 K to 200 000 K and from $\log g = 6.0$ to $\log g = 9$. From 6 000 K to 20 000 K, a grid with 250 K temperature steps was set up, covering the range of $7.5 \leq \log g \leq 8.5$ in 0.1 dex intervals, extending up to 9.0 and down to 7.0, for the models with $T_{\rm eff} \leq$ 10 000 K down to 6.0, in 0.25 dex increments. Convective flux was taken into account in these models following the standard mixing length approximation (Böhm-Vitense 1958). We used ML2 models described by Koester et al. (1994) with a mixing length $\alpha = 0.6$ according to their notation, and following the results of Bergeron et al. (1995), and Koester & Vauclair (1997). Input physics and numerical techniques are the same as used by

FKB and are described in detail therein, although the program code is evolving continuously and not identical to that used by FKB.

4.2. Determination of $T_{\rm eff}$ and $\log g$

The best fitting model was determined by a χ^2 routine, minimizing the differences between observed spectra and models (obtained with a bilinear interpolation in the grid) in the region of the Balmer lines. The width of these regions was set according to line widths of each spectrum. These were estimated from visual inspection or a tentative fit. For the coolest stars we used 350 Å wide segments for the Hα and Hβ lines, while the higher lines up to H8, if available, are already overlapping and were thus handled by one contiguous segment from 170 Å redwards of Hγ on. For intermediate temperatures 160 Å to 200 Å wide bandpasses were chosen for Hα to Hγ and a limit of 80 Å to the red of Hδ for the higher lines. The hottest stars, above approximately 50 000 K, were fitted within 100 – 120 Å wide segments around Hα to Hδ, the last of which was extended to Hϵ for those spectra that could provide sufficient S/N at the blue end. Fig. 1 shows exactly the fitted spectral ranges for each object.

To derive the noise of the spectra as a function of λ within each of these segments, the random errors in the adjacent continuum were empirically determined by the following procedure: A smoothed continuum was calculated by averaging the spectrum with a fourth-order Savitzky-Golay filter in a moving window of 31 pixels full width. The continuum noise was taken to be the mean deviation of the observed spectrum from this smoothed spectrum. The noise within the lines was then obtained by bilinear interpolation of the variances from the neighbouring continuum regions.

For each point in ($T_{\rm eff}$, $\log g$) to be fitted to the observation, a theoretical spectrum was interpolated from the grid as described above and folded with a Gaussian of width equivalent to the instrumental resolution. Due to the variable observing conditions the flux calibration of the spectra was not reliable enough to allow the use of the continuum slope for temperature determinations. Similar to the method for determining the errors, the spectrum was sampled by a number of regions of the continuum near to the Balmer lines. The mean flux in each region was linearly interpolated to adjust the model flux. The total χ^2 was then calculated as the sum of the χ^2s of all line regions chosen for the fit. The best-fit values of $T_{\rm eff}$ and $\log g$ were found by an implementation of the Levenberg-Marquard algorithm (cf. Press et al. 1992).

Four stars have been observed twice during the different observation campaigns. With the exception of KUV 03561+0807, where the 3.5m spectrum was discarded on account of its very poor S/N, we have calculated mean values of $T_{\rm eff}$ and $\log g$ from the results of both spectra for these, weighted with the inverse of the respective internal errors. Six of the hottest stars have also been reobserved at high resolution and good signal-to-noise in June 1996, with usually two observations each. For these we used only the pair of newer spectra. These averaged values have been used for the further calculations. The results of the individual observations are displayed for comparison in Table 5.

4.3. Masses, luminosities and distances

Knowledge of the values of $T_{\rm eff}$ and $\log g$ allows the determination of the the stellar mass and the radius from a theoretical mass-radius relation. The effective temperature enters the relation, since deviations from the Hamada-Salpeter-Relation for fully degenerate, zero-temperature cores become important at higher temperatures. The appropriate mass-radius relation has been taken from a set of evolutionary models by Wood (1994,1995) with pure carbon cores, helium layers of $M_{\rm He} = 10^{-2} M_\star$ and additional thick hydrogen layers of $M_{\rm H} = 10^{-4} M_\star$. Cooling tracks for masses from 0.4 to 1.1 $\rm M_\odot$, with intervals of 0.1 $\rm M_\odot$ have been employed in this work.

We also used the information on the energy distribution in the model spectra to calculate several standard colours as well as the total flux from theoretical filter transmission curves. From the radii determined from the mass-radius relation, luminosities and absolute V and B magnitudes could then be derived. The latter, in combination with the magnitudes measured on the objective prism plates, provided distance moduli for the sample.

4.4. Errors

The standard deviations of the parameters listed in Table 4 are given as the formal errors from the covariance matrix of the fit, which is a somewhat simplified approach to determine the statistical errors and cannot reflect all possible systematic errors. For spectra with good signal-to-noise, the actual uncertainties are dominated by external errors arising from data acquisition and reduction, and limitations of the theoretical models.

Most of our objects have been originally discovered by this survey, so that the overlap with other surveys is small. Most stars have also been only observed once during our program. This allows only a check of the external errors on a subsample of stars. We list the results of all independent observations in Table 5 and have taken the unweighted mean of all available observations for each star listed there (this implies that all observations yielded a priori equally precise results, but for lack of another independent measure of errors we have to make this assumption). The absolute and relative errors in $T_{\rm eff}$ and errors in $\log g$ are given for the single observations.

Generally the external errors turn out to be by a factor of two to five larger than the internal errors. The average relative external error of all observations is $\langle \sigma(T_{\rm eff})/T_{\rm eff} \rangle = 0.022$ in temperature , and $\langle \sigma(\log g) \rangle = 0.1$ in gravity.

A notable exception is RE J 1820+580, for which rather discrepant results were obtained by all of the various studies. The errors tend to increase at higher temperatures. If the stars with $T_{\rm eff} > 70\,000$ K are omitted, the mean error drops to 1.73% in temperature and 0.086 in $\log g$. These values should be regarded the lower limits for all observations with good signal-to-noise.

The five very hot stars reobserved in 1996 at high resolution and under very good conditions still show considerable variation

Table 4. Stellar parameters, derived masses, radii, absolute magnitudes and distances for 79 white dwarfs.

Name	$T_{\rm eff}$(K)	$\sigma(T_{\rm eff})$	$\log g$	$\sigma(\log g)$	$M_\star$ [$M_\odot$]	$\sigma(M_\star)$	$R_\star$ [0.01$R_\odot$]	$\sigma(R_\star)$	M_B	$\sigma(M_B)$	B	$D_{\rm lum}$(pc)	Notes
HS 0008+3302	10300	180	8.35	0.29	0.83	0.18	1.00	0.21	$12\overset{m}{.}8$	0.05	$17\overset{m}{.}5$	85	C
HS 0009+1621	16100	830	7.55	0.18	0.40	0.08	1.76	0.19	$10\overset{m}{.}5$	0.09	$17\overset{m}{.}2$	210	CX
HS 0026+3114	53600	420	7.57	0.03	0.53	0.01	1.97	0.04	$8\overset{m}{.}1$	0.01	$15\overset{m}{.}6$	310	
GD 8	48900	240	7.85	0.02	0.62	0.01	1.55	0.02	$8\overset{m}{.}4$	0.00	$14\overset{m}{.}6$	150	X
HS 0047+0716	14800	350	7.91	0.08	0.56	0.05	1.38	0.07	$11\overset{m}{.}2$	0.04	$16\overset{m}{.}7$	120	C
HS 0129+0511	13100	330	7.83	0.05	0.52	0.03	1.45	0.05	$11\overset{m}{.}4$	0.05	$15\overset{m}{.}9$	75	Z
HS 0130+0156	37000	1800	7.12	0.26	0.35	0.08	2.63	0.42	$7\overset{m}{.}1$	0.07	$16\overset{m}{.}0$	410	M
HS 0130+0800	13100	310	7.69	0.06	0.45	0.03	1.58	0.05	$11\overset{m}{.}2$	0.04	$16\overset{m}{.}4$	110	Z
HS 0146+0723	25000	1800	8.27	0.22	0.80	0.14	1.08	0.18	$10\overset{m}{.}7$	0.13	$17\overset{m}{.}3$	210	C
Feige-17	20600	200	7.72	0.04	0.49	0.02	1.60	0.04	$10\overset{m}{.}2$	0.02	$14\overset{m}{.}7$	75	
HS 0210+1629	16900	230	7.91	0.05	0.57	0.03	1.38	0.04	$10\overset{m}{.}9$	0.02	$16\overset{m}{.}4$	120	
HS 0235+0655	11420	60	7.93	0.05	0.56	0.03	1.35	0.04	$11\overset{m}{.}8$	0.01	$16\overset{m}{.}8$	95	Z
HS 0235+0514	16000	1400	7.63	0.31	0.43	0.14	1.66	0.31	$10\overset{m}{.}7$	0.15	$17\overset{m}{.}8$	260	N
GD 41	37600	160	7.72	0.03	0.54	0.01	1.68	0.03	$8\overset{m}{.}9$	0.01	$14\overset{m}{.}6$	140	X
HS 0348+2803	17800	860	7.93	0.16	0.58	0.09	1.37	0.15	$10\overset{m}{.}9$	0.08	$17\overset{m}{.}1$	170	C
KUV 03520+0500	36400	170	8.85	0.04	1.12	0.02	0.66	0.03	$10\overset{m}{.}9$	0.01	$15\overset{m}{.}8$	90	M
KUV 03561+0807	41600	830	7.61	0.11	0.51	0.04	1.85	0.15	$8\overset{m}{.}4$	0.02	$15\overset{m}{.}4$	240	C
HS 0401+0001	50900	670	7.70	0.05	0.57	0.02	1.75	0.07	$8\overset{m}{.}3$	0.01	$17\overset{m}{.}1$	550	
HS 0421+0342	31700	790	8.05	0.20	0.68	0.11	1.29	0.18	$9\overset{m}{.}8$	0.05	$15\overset{m}{.}9$	170	C
HS 0424+0141	48000	1100	7.78	0.09	0.59	0.04	1.64	0.11	$8\overset{m}{.}4$	0.02	$15\overset{m}{.}6$	250	
HS 0503+0154	57400	460	7.86	0.03	0.65	0.02	1.56	0.04	$8\overset{m}{.}7$	0.01	$15\overset{m}{.}2$	210	
HS 0507+0434 B	11720	40	7.90	0.03	0.55	0.02	1.38	0.02	$11\overset{m}{.}7$	0.01	$15\overset{m}{.}6$	55	Z
HS 0507+0434 A	20030	70	7.98	0.01	0.62	0.01	1.33	0.01	$10\overset{m}{.}7$	0.01	$14\overset{m}{.}3$	50	
HS 0615+6535	98000	5500	7.07	0.15	0.55	0.04	3.55	0.53	$6\overset{m}{.}6$	0.05	$15\overset{m}{.}2$	600	T
HS 0641+6528	17700	250	8.07	0.06	0.66	0.03	1.24	0.04	$11\overset{m}{.}1$	0.02	$16\overset{m}{.}2$	100	
HS 0727+6915	12100	250	8.29	0.14	0.79	0.09	1.06	0.11	$12\overset{m}{.}2$	0.04	$16\overset{m}{.}9$	85	Z
HS 0742+2306	60000	660	7.66	0.04	0.58	0.02	1.85	0.06	$8\overset{m}{.}4$	0.01	$17\overset{m}{.}0$	600	
HS 0841+4547	29000	1900	8.19	0.34	0.76	0.20	1.15	0.29	$10\overset{m}{.}2$	0.14	$15\overset{m}{.}7$	120	C
HS 0943+4724	16000	2200	8.75	0.26	1.07	0.14	0.72	0.18	$12\overset{m}{.}4$	0.23	$17\overset{m}{.}8$	120	ZN
HS 0943+4852	19000	3000	7.90	0.50	0.57	0.27	1.40	0.49	$10\overset{m}{.}7$	0.27	$19\overset{m}{.}0$	450	N
HS 0946+4848	11700	310	8.69	0.35	1.04	0.20	0.76	0.24	$13\overset{m}{.}0$	0.07	$17\overset{m}{.}6$	80	Z
HS 0946+5009	30300	290	7.99	0.07	0.65	0.04	1.34	0.07	$9\overset{m}{.}0$	0.02	$16\overset{m}{.}6$	230	
HS 0949+4935	15000	1400	8.39	0.16	0.86	0.11	0.98	0.12	$11\overset{m}{.}9$	0.16	$18\overset{m}{.}4$	190	Z
HS 0951+3620	65000	1500	7.66	0.08	0.59	0.03	1.88	0.12	$8\overset{m}{.}4$	0.02	$17\overset{m}{.}5$	800	
HS 1001+4651	18100	230	7.89	0.05	0.56	0.03	1.40	0.04	$10\overset{m}{.}8$	0.02	$16\overset{m}{.}4$	130	
HS 1002+4518	35800	810	7.99	0.16	0.66	0.09	1.36	0.16	$9\overset{m}{.}2$	0.04	$16\overset{m}{.}9$	310	C
HS 1003+4852	16100	490	8.19	0.10	0.73	0.07	1.14	0.08	$11\overset{m}{.}5$	0.05	$16\overset{m}{.}0$	80	
HS 1110+2150	46600	380	7.65	0.04	0.53	0.02	1.81	0.05	$8\overset{m}{.}5$	0.01	$17\overset{m}{.}0$	500	
Ton 82	20100	390	7.48	0.06	0.39	0.03	1.88	0.06	$9\overset{m}{.}7$	0.03	$15\overset{m}{.}8$	150	M
GD 148	14700	160	7.96	0.03	0.59	0.02	1.33	0.03	$11\overset{m}{.}3$	0.02	$14\overset{m}{.}7$	45	
PG 1234+482	56000	780	7.84	0.05	0.63	0.02	1.58	0.06	$8\overset{m}{.}6$	0.01	$14\overset{m}{.}5$	150	
HS 1241+4821	14800	500	8.54	0.05	0.95	0.03	0.87	0.03	$12\overset{m}{.}3$	0.06	$17\overset{m}{.}1$	90	
GD 348	9640	20	7.91	0.04	0.55	0.02	1.36	0.03	$12\overset{m}{.}4$	0.01	$14\overset{m}{.}7$	30	
PG 1541+650	12000	70	7.79	0.04	0.49	0.02	1.48	0.03	$11\overset{m}{.}5$	0.01	$15\overset{m}{.}7$	65	Z
HS 1556+6025	17500	150	8.03	0.03	0.64	0.02	1.28	0.03	$11\overset{m}{.}0$	0.01	$16\overset{m}{.}9$	140	
HS 1610+6149	10670	30	7.96	0.05	0.58	0.03	1.32	0.04	$12\overset{m}{.}1$	0.01	$16\overset{m}{.}8$	85	Z
HS 1619+6443	30110	40	7.82	0.01	0.56	0.01	1.53	0.01	$9\overset{m}{.}3$	0.00	$15\overset{m}{.}4$	150	X
HS 1627+7436	13900	210	8.10	0.03	0.67	0.02	1.21	0.02	$11\overset{m}{.}7$	0.03	$15\overset{m}{.}7$	60	
HS 1641+7132	11600	80	7.98	0.06	0.59	0.04	1.31	0.05	$11\overset{m}{.}9$	0.02	$16\overset{m}{.}7$	90	Z
HS 1650+7229	53000	1600	7.61	0.12	0.54	0.04	1.90	0.18	$8\overset{m}{.}1$	0.03	$17\overset{m}{.}6$	750	
HS 1653+7753	29400	210	7.15	0.05	0.32	0.02	2.46	0.06	$8\overset{m}{.}6$	0.02	$14\overset{m}{.}8$	180	M
HS 1703+6315 A	16100	360	7.68	0.08	0.45	0.04	1.61	0.09	$10\overset{m}{.}7$	0.04	$16\overset{m}{.}3$	130	
HS 1729+7735	13800	290	7.69	0.07	0.45	0.03	1.58	0.07	$11\overset{m}{.}1$	0.04	$16\overset{m}{.}0$	95	
HS 1730+7844	13400	390	7.68	0.06	0.44	0.03	1.60	0.06	$11\overset{m}{.}1$	0.05	$16\overset{m}{.}0$	90	
HS 1745+6043	35600	220	8.68	0.04	1.05	0.02	0.78	0.03	$10\overset{m}{.}6$	0.01	$16\overset{m}{.}0$	120	
HS 1749+7145	76900	550	7.56	0.03	0.59	0.01	2.10	0.04	$7\overset{m}{.}4$	0.01	$15\overset{m}{.}7$	410	
HS 1817+7852	31200	440	7.95	0.12	0.63	0.06	1.39	0.12	$9\overset{m}{.}6$	0.03	$16\overset{m}{.}6$	240	
RE J 1820+580	45900	170	8.00	0.02	0.68	0.01	1.37	0.02	$9\overset{m}{.}8$	0.00	$13\overset{m}{.}3$	70	
HS 1822+7452	9690	50	7.97	0.15	0.59	0.09	1.31	0.13	$12\overset{m}{.}5$	0.02	$17\overset{m}{.}2$	85	
HS 1827+7753	75800	610	7.68	0.03	0.62	0.01	1.89	0.05	$7\overset{m}{.}8$	0.01	$15\overset{m}{.}7$	370	X
KUV 18453+6819	37700	210	8.24	0.04	0.80	0.02	1.13	0.03	$9\overset{m}{.}6$	0.01	$14\overset{m}{.}8$	100	
RE J 1918+595	32670	80	7.98	0.02	0.65	0.01	1.36	0.02	$9\overset{m}{.}0$	0.00	$14\overset{m}{.}3$	85	
HS 1938+6902	15800	200	7.52	0.05	0.39	0.02	1.79	0.05	$10\overset{m}{.}5$	0.02	$16\overset{m}{.}3$	140	M
HS 2058+0823	36830	70	7.86	0.01	0.60	0.01	1.50	0.01	$9\overset{m}{.}6$	0.00	$14\overset{m}{.}7$	130	
PG 2120+055	36600	200	7.94	0.03	0.63	0.02	1.41	0.03	$9\overset{m}{.}1$	0.01	$15\overset{m}{.}8$	200	
HS 2157+8153	10700	40	8.71	0.08	1.05	0.04	0.75	0.05	$13\overset{m}{.}3$	0.01	$16\overset{m}{.}0$	35	Z
HS 2210+1130	29900	300	7.99	0.08	0.65	0.04	1.34	0.07	$9\overset{m}{.}3$	0.02	$16\overset{m}{.}8$	250	
PG 2220+134	22600	910	8.81	0.16	1.10	0.08	0.68	0.11	$11\overset{m}{.}9$	0.08	$15\overset{m}{.}5$	50	C
HS 2234+8352	13500	220	7.88	0.04	0.54	0.02	1.40	0.03	$11\overset{m}{.}4$	0.03	$16\overset{m}{.}0$	80	
HS 2235+0813	37100	460	7.82	0.08	0.58	0.04	1.55	0.09	$9\overset{m}{.}9$	0.02	$15\overset{m}{.}3$	170	
HS 2236+3118	35200	110	7.49	0.02	0.45	0.01	1.99	0.03	$8\overset{m}{.}2$	0.00	$14\overset{m}{.}1$	120	
PG 2239+082	22300	250	7.80	0.04	0.53	0.02	1.52	0.03	$10\overset{m}{.}2$	0.02	$16\overset{m}{.}5$	180	
HS 2240+1234 B	14000	540	8.17	0.08	0.72	0.05	1.15	0.06	$11\overset{m}{.}8$	0.07	$16\overset{m}{.}7$	95	
HS 2240+1234 A	15300	170	7.97	0.04	0.60	0.03	1.33	0.03	$11\overset{m}{.}2$	0.02	$16\overset{m}{.}4$	100	

Table 4. (continued)

Name	$T_{\rm eff}$(K)	$\sigma(T_{\rm eff})$	$\log g$	$\sigma(\log g)$	$M_\star$ [$M_\odot$]	$\sigma(M_\star)$	$R_\star$ [0.01$R_\odot$]	$\sigma(R_\star)$	M_B	$\sigma(M_B)$	B	$D_{\rm lum}$(pc)	Notes
HS 2244+0305	72000	1600	7.78	0.08	0.65	0.03	1.72	0.11	$8\overset{\rm m}{.}4$	0.02	$16\overset{\rm m}{.}2$	410	
HS 2246+0640	98000	1700	7.04	0.05	0.54	0.02	3.68	0.18	$6\overset{\rm m}{.}8$	0.01	$16\overset{\rm m}{.}8$	1350	T
PG 2308+050	37600	250	7.62	0.04	0.50	0.02	1.81	0.05	$8\overset{\rm m}{.}2$	0.01	$15\overset{\rm m}{.}6$	240	
HS 2330+0556	12800	820	7.68	0.13	0.44	0.06	1.60	0.13	$11\overset{\rm m}{.}2$	0.12	$17\overset{\rm m}{.}2$	150	Z
PG 2353+027	63200	600	7.57	0.04	0.55	0.01	2.03	0.06	$7\overset{\rm m}{.}0$	0.01	$14\overset{\rm m}{.}8$	240	

Quality flags: C: Bad wavelength calibration or very low resolution; X: Reduced $\chi^2 > 2.0$; N: Extremely noisy spectrum; M: Mass extrapolated from the set of cooling tracks; T: $T_{\rm eff}$ extrapolated from cooling tracks; F: Flux (M_B) extrapolated from model grid; Z: ZZ Ceti-candidate

Table 5. Comparison of our results with other work and of multiple observations in this study, and deviations of our results from the mean

Object	$T_{\rm eff}$	σ	$\log g$	σ	Observation	Source	$T_{\rm eff}$	σ	$\log g$	σ	$\langle T_{\rm eff}\rangle$	$\langle \log g\rangle$	$\Delta T_{\rm eff}$	$\frac{100\Delta T_{\rm eff}}{\langle T_{\rm eff}\rangle}$	$\Delta \log g$
HS0026+3144	52600	500	7.57	.04	08/93	01/95	55100	740	7.56	.05	53850	7.56	1250	2.32	.01
GD 8	48900	240	7.85	.02	08/93	FKB	48655	520	7.74	.05	48777	7.79	120	0.25	.11
GD 41	37600	160	7.72	.03	09/92	FKB	35082	257	7.64	.06	36094	7.71	1500	4.13	.013
						V97	35600	200	7.76	.06					
KUV03520+0500	36700	190	8.89	.03	10/90	08/92	36000	340	8.72	.07	36350	8.80	350	0.96	.17
HS0507+0434B	11720	40	7.90	.03	09/92	J98	11900	300	8.00	.05	11810	7.95	90	0.76	.10
HS0507+0434A	20030	70	7.98	.01	09/92	J98	20220	50	7.99	.05	20125	7.99	95	0.47	.01
GD 148	14700	160	7.96	.03	01/89	BSL	14700	200	7.90	.04	14700	7.93	0	0.00	.06
PG1234+482	56000	780	7.84	.05	01/89	FKB	56382	493	7.67	.03	56461	7.81	460	0.82	.033
						B95	57000	700	7.91	.04					
GD 348	9640	20	7.91	.04	06/91	K95	9831	42	8.13	.04	9735	8.02	95	0.98	.11
PG1620+648	30600	110	7.85	.03	06/91	B95	30800	100	7.75	.03	30480	7.79	120	0.39	.06
	30030	40	7.78	.01	06/96	B95	30800	100	7.75	.03	30480	7.79	450	1.48	.01
HS1749+7145	75400	720	7.59	.03	06/96a	06/96b	78500	830	7.53	.03	76950	7.56	1550	2.01	.03
REJ1820+580	45900	170	8.00	.02	06/96	FKB	49610	626	7.86	.06	46035	7.82	140	0.29	.177
						M97	45330	850	7.73	.07					
						N98	43300	260	7.70	.03					
HS1827+7753	73200	840	7.56	.04	06/96a	06/96b	78500	880	7.78	.04	75850	7.67	2650	3.49	.11
REJ1918+595	32700	80	7.98	.02	06/96	V97	33000	200	7.90	.05	32850	7.94	150	0.46	.04
KUV18453+6819	37700	210	8.24	.04	06/91	V97	37400	300	8.24	.04	36900	8.21	800	2.13	.03
						N98	35600	200	8.15	.03					
HS2058+0853	36870	90	7.87	.02	06/96a	06/96b	36800	110	7.84	.02	36835	7.86	35	0.10	.015
PG2120+055	36600	200	7.94	.03	09/92	FKB	34155	398	7.80	.10	35377	7.87	1220	3.45	.07
PG2239+082	22300	250	7.80	.04	06/91	FKB	21862	160	7.72	.03	22081	7.76	220	1.00	.04
HS2246+0640	94000	1800	7.23	.06	06/96b	06/96b	105000	3500	6.75	.09	99500	6.99	5500	5.53	.24
PG2353+026	62300	760	7.59	.05	06/96a	FKB	62013	760	7.74	.04	62840	7.62	540	0.86	.03
	64200	950	7.54	.06	06/96b	FKB	62013	760	7.74	.04	62840	7.62	1040	2.16	.08

$\langle T_{\rm eff}\rangle$ and $\langle \log g\rangle$ averaged over all observations listed here. Sources: BSL: Bergeron et al. 1992; FKB: Finley et al. 1997; V97: Vennes et al. 1997; J98: Jordan et al. 1998; N98: Napiwotzki (priv. comm.); B94: Bergeron et al. 1994; K95: Kepler et al. 1995; M97: Marsh et al. 1997; other: years of multiple observations (this work), 93 was a simultaneous observation at the 2.2m and 3.5m telescopes.

of the parameters fitted for different spectra; moreover even fits for one and the same spectrum would give different results depending on the number of lines included. This is mainly due to the weakness of the Balmer lines at these temperatures (see Fig. 1), but additionally the effects of photospheric trace elements and NLTE to be discussed in Sect. 5 may come into play.

For several stars with observations of poorer S/N the errors might also considerably exceed both the average external error given above and the quoted internal errors: Six spectra were lacking a satisfactory wavelength calibration, on three others we failed to achieve a fit with a reasonable χ^2, and two of the remainder had extremely bad signal-to-noise ratios. In all these cases, marked by respective flags in Table 4 the formal errors would not provide a reliable measure of the true uncertainties. Temperature estimates for these stars might be wrong by more than 20 %, and $\log g$ determinations are even more uncertain. This could be inferred from tests in which individual lines had been omitted from the analysis, which could lead to deviations of up to 0.5 – 1.0 dex in the solution for $\log g$. Consequently, mass estimations and distances might be wrong by a factor of two for the stars denoted accordingly.

Another problem in temperature determination arises for the stars with $10\,000\,{\rm K} \leq T_{\rm eff} \leq 20\,000\,{\rm K}$ as the Balmer line strength varies very slowly near its maximum at about 12 000 K, and temperature changes can also be partially compensated by changes in $\log g$ in this area. The temperature solutions are particularly sensitive on the starting values for the fit algorithm. We could e. g. obtain fits for HS1003+4852 at $T_{\rm eff} = 13\,000\,{\rm K}$ and $T_{\rm eff} = 14\,500\,{\rm K}$ that gave a reduced χ^2 only a few percent higher than at the absolute minimum. Other stars for which multiple solutions have been found are HS 2157+8153 (19 750 K, 8.3 vs. 10 700 K, 8.7), Ton 82 (9900 K, 8.1 vs. 20 100 K, 7.5), HS 1938+6902 (10 600 K, 7.5 vs. 15 800 K, 7.5) and HS 1556+6025 (11 200 K, 8.3 vs. 17 500 K, 8.0). The continuum slope of the optical spectrum, on the other hand, is very sensitive to such a temperature difference. Except for Ton 82 these spectra were obtained in June 1996 at excellent conditions giving some trust in the fluxing of the spectra. The flux distributions are in agreement with the high $T_{\rm eff}$ solutions for HS 1556+6025 and HS 1938+6902 and support the low $T_{\rm eff}$ solution for HS 2157+8153. For Ton 82 we could not rely on the fluxes from the slit spectrum, while inspection of the slope of the objective prism spectra and comparison with objects with a re-

liable temperature determination support the high $T_{\rm eff}$ solution and do also confirm the temperatures for the other stars.

The calculations of mass and radius are based solely on the mass-radius relation, and therefore no independent errors can be given for these values. As the dependence of the $M-R$ relation of $T_{\rm eff}$ becomes only significant at the very highest temperatures, it is mainly the error in $\log g$ that enters in the mass uncertainty, as can be seen by the intersections of the error bars with the isobaric lines in Fig. 2. It might then surprise that the quoted mass errors for some stars are quite small in relation to the errors in $\log g$, but this is can be explained by the shape of the $M-R$ relation. As an example we will consider first a relatively cool white dwarf of moderate mass, with $T_{\rm eff} = 20\,000$ K and $\log g = 8$. Interpolation of the cooling tracks from Wood (1994) returns a mass of $0.627\mathrm{M}_\odot$ and a mass–radius relation of $R \propto M^{-\frac{3}{4}}$ for such an object. From $g = \frac{GM}{R^2}$ we immediately obtain the relation $g = GM^{\frac{5}{2}}$, or $\log M = \frac{2}{5}\log g - \log G$ and thus $\sigma_M = \ln 10 \cdot M \cdot \frac{2}{5}\sigma_{\log g} \approx 0.92 M \sigma_{\log g}$. A $\sigma_{\log g} = 0.08$ adopted above as external error corresponds then to $\sigma_M = 0.049$. A $T_{\rm eff} = 60\,000$ K, $\log g = 7$ star, in comparison, has a mass of $0.392\mathrm{M}_\odot$ and a distinctively steeper mass–radius relation $R \propto M^{-\frac{4}{3}}$ (with the exponent even falling to -2 and below for temperatures as high as 80 000 K), so error propagation changes accordingly to $\sigma_M = \ln 10 \cdot M \cdot \frac{3}{11}\sigma_{\log g} \approx 0.63 M \sigma_{\log g}$. An error of $\sigma_{\log g} = 0.08$ translates to only $\sigma_M = 0.024$ in this case. All of these estimates are of course depending on the validity of the cooling models.

The same errors affect the absolute magnitudes calculated from radii and theoretical flux, but the errors in the distance moduli are in most cases dominated by the photometric error of the apparent B magnitudes of $0\overset{\rm m}{.}5$, leading to an error in the distance determination of about 30%. There may exist further systematic errors in the connection of the theoretical flux to the standard magnitude system, though.

From the external consistency checks available we conclude that the the temperatures determined for our sample are of similar accuracy as in other spectroscopical studies, although $\log g$ seems to be somewhat less accurate.

4.5. Results

The temperatures found for the Hamburg Survey DAs span a wide range from below 10 000 K up to about 100 000 K. Among these are some of the hottest DA white dwarfs known to date, which will be discussed in detail in the following Sect. (5). Some of the cooler stars deserve closer attention as well, since their temperatures fall close to the position of the ZZ Ceti strip for non-radial pulsationary instability. With ML2/$\alpha = 0.6$, Bergeron et al. (1995) specified 11 160 – 12 460 K as the range of temperatures for pulsating DA white dwarfs. We found 13 stars that lie inside the instability strip within 2 σ of either internal or an average external error of 250 K, whichever is greater. These are denoted in Table 4 as possible ZZ Ceti variables. The ZZ Ceti strip coincides with the temperature range of maximum

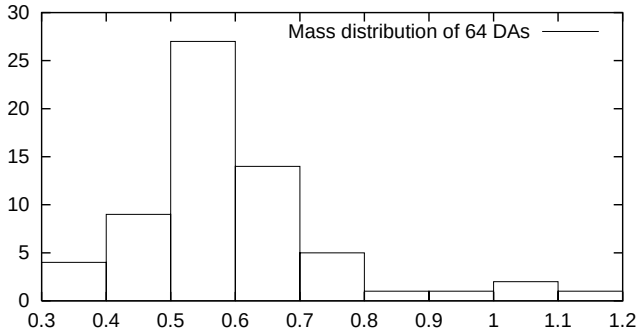

Fig. 3. Mass distribution for the subsample of 64 white dwarfs with good stellar parameters, i.e. omitting those marked by C, X or N in Table 4

Balmer line strength, and accordingly some uncertainty about the correct solutions for $T_{\rm eff}$ remains, as described above.

HS 0507+0434 B has already been confirmed as a ZZ Ceti variable by Jordan et al. (1998), the results being quoted in Table 5. They also reported the other double degenerate from our sample, HS 2240+1234, but this analysis (which gives slightly lower temperatures) is based on the same observation as ours. We also note here that a third star in the sample, HS 1703+6315, has a visual companion as well, of which we could not obtain a good spectrum. A comparison with the POSS I shows, however, that the relative position of both stars has changed by several arcseconds since 1953; the possibility of a physical binary can therefore be excluded.

At first glance, our sample contains a relatively large number of high mass stars, seven stars having masses $> 0.9\,\mathrm{M}_\odot$. Four of these belong to the objects with uncertain parameters, though; this effect is caused by the fact that spectra with uncertain wavelength calibration tend to be fitted at a higher $\log g$ as the line positions are not well determined. After discarding these spectra, we are left with three stars of masses in excess of $1\ \mathrm{M}_\odot$, HS 1745+6043, KUV 03520+0500 and HS 2157+8153 (provided that our choice of the temperature solution for the latter is correct). For the subsample of 64 stars with reliable spectroscopic data (Fig. 3) the mean mass $\langle M \rangle = 0.605\mathrm{M}_\odot$, with a dispersion of $0.15\ \mathrm{M}_\odot$ is slightly higher than in other samples.

On the other hand we find several stars near to or below the lower mass limit expected for single white dwarf evolution. At least three have masses significantly less than $0.45\ \mathrm{M}_\odot$. The currently favoured explanation for the formation of white dwarfs with masses $\lesssim 0.45\mathrm{M}_\odot$ is close binary evolution with a common envelope phase (Iben & Tutukov 1986). Marsh et al. (1995) have demonstrated in a study of seven low-mass white dwarfs from the BSL sample that the frequency of close binary detections is high (five systems) among these stars.

5. Observations at shorter wavelengths: the hot sample

Our study resulted in the discovery of a considerable number of very hot DAs that provide interesting targets for observations

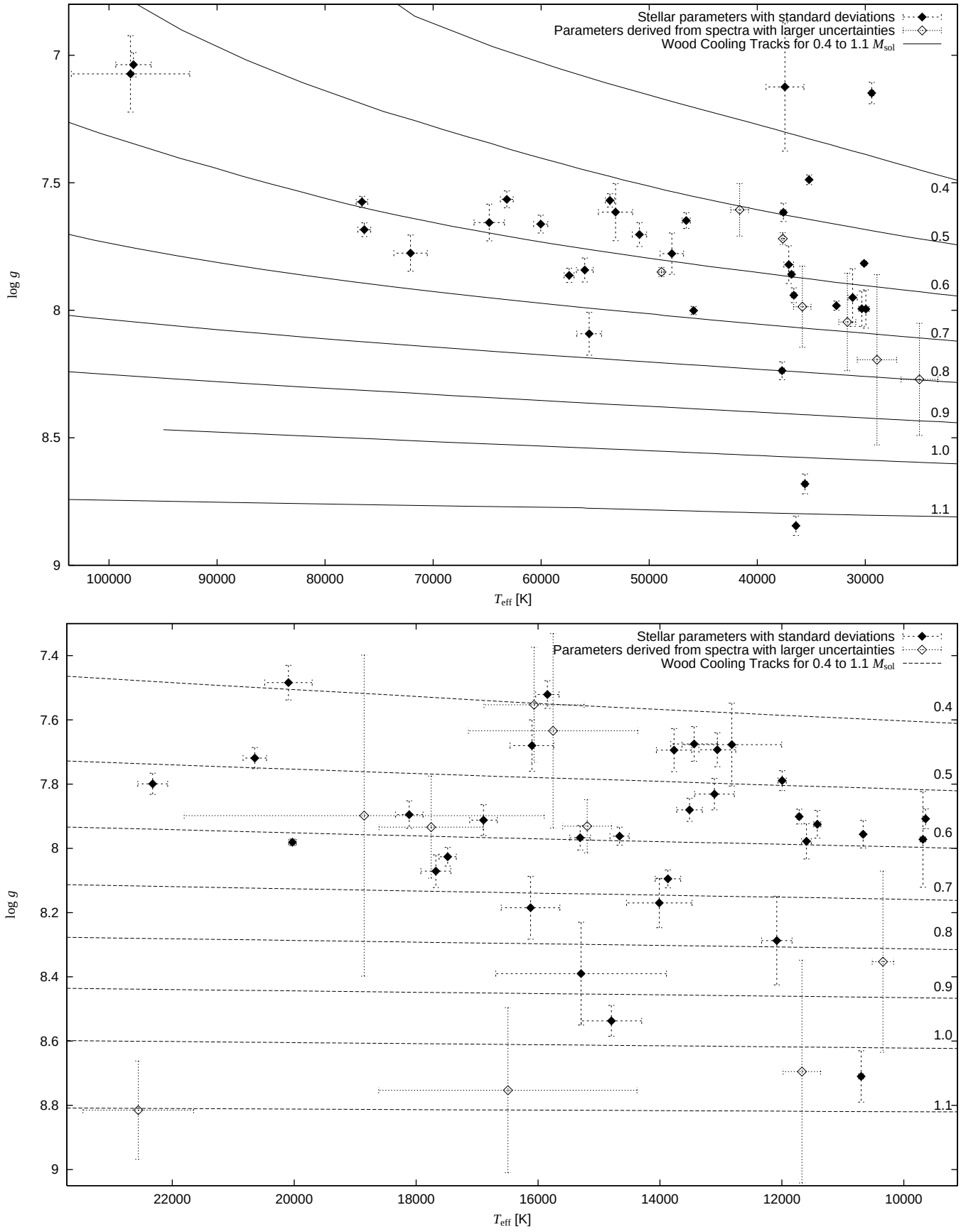

Fig. 2. Distribution of effective temperatures and surface gravities of all 79 white dwarfs against Wood (1994) cooling tracks. The observations with larger errors in the parameters, i.e. those marked by C, X or N in Table 4 are displayed as open symbols

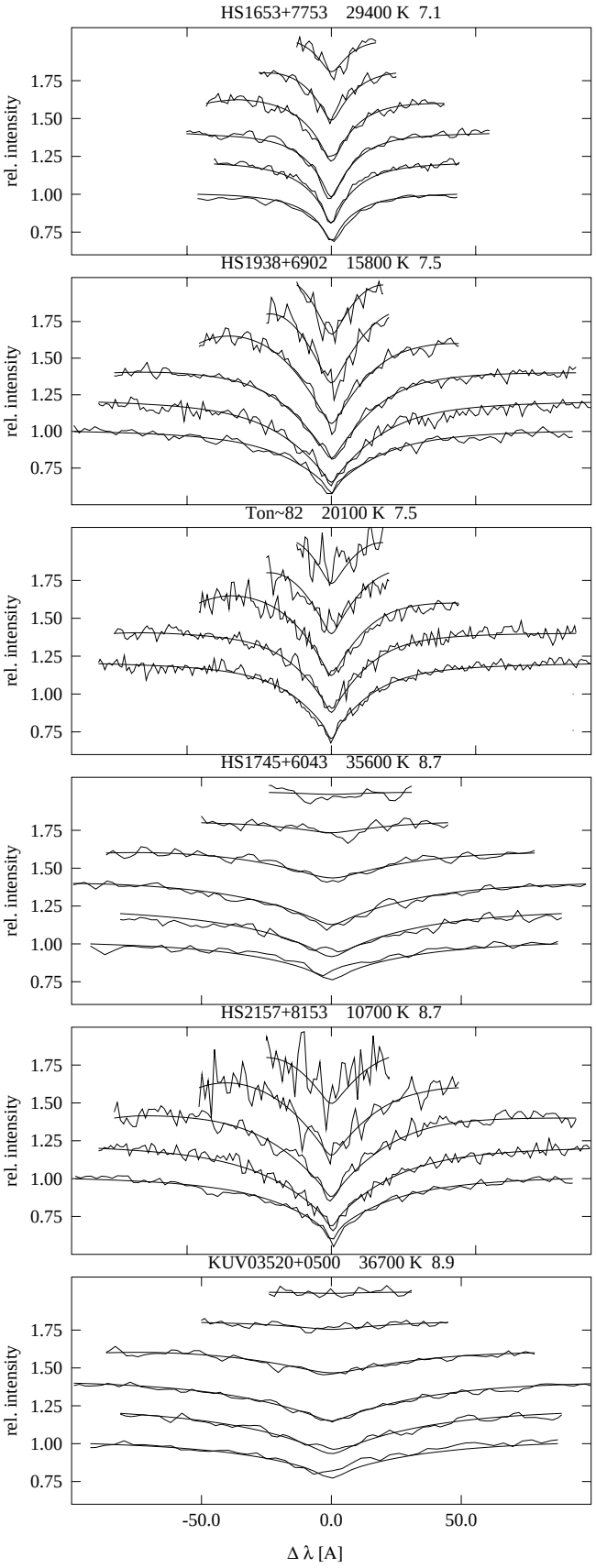

Fig. 4. Fits of the three putative low-mass white dwarfs and the three high-mass suspects

in the UV and EUV. 13 stars from the list have optically determined $T_{\rm eff} \leq 50\,000$ K, at least five more are found to lie in the range from 40 000 K to 50 000 K. The number of DA white dwarfs with spectroscopically determined $T_{\rm eff} > 50\,000$ K to date is 44 (Bergeron et al. 1994, Marsh et al. 1997,Vennes et al. 1997, FKB), which is increased by the number of eleven newly discovered stars from this work.

Since most of the photospheric flux of hot white dwarfs is emitted in the soft X-ray and EUV, the four hottest stars have been observed with the ROSAT HRI detector (PI: S. Jordan). None of them could be detected, but the absence of soft X-ray emission at this level suggests the presence of metals in the photospheres of these white dwarfs: Table 6 lists the four stars with their upper limits on the count rate in the HRI band. First the X-ray flux predicted for these stars by our pure hydrogen model atmospheres was used to calculate synthetic count rates for a range of H I column densities. Thus we determined the amount of interstellar H I required to match the ROSAT upper limits (B. Wolff, priv. comm.). If we compare these values with the measured interstellar column density of galactic neutral hydrogen at the positions of the four stars as given by the Bell Laboratories 21 cm survey (Stark et al.1992), we find these to be too small by at least $\sim 10^{21}{\rm cm}^{-2}$, or a factor of three. This corresponds to a discrepancy between the observed and predicted count rates of more than an order of magnitude in all cases. Hence we conclude that the soft X-ray/EUV deficit can not be caused entirely by H I absorption and the stars must contain metal absorbers in their photospheres.

This conclusion fits into the picture that radiative levitation leads to significant amounts of metals (especially iron) in the atmospheres of all hot DA white dwarfs above 50 000 K (e.g. Barstow et al. 1993, Wolff et al. 1996, 1998). We find this interpretation confirmed by the three stars in our sample with $T_{\rm eff}$ between 30 000 and 50 000 K that have been detected as EUV-sources (RE J 1820+580, RE J 1918+595 and HS 1745+6043). Due to the blanketing effect one has to take into account that our $T_{\rm eff}$ values determined with the help of pure hydrogen atmospheres are upper limits to the effective temperatures. If metal absorbers are present in the atmospheres the flux reduction in the EUV is compensated by a higher flux in the UV and optical at a given effective temperature (i.e. given total flux). In the case of the hot DA star G 191B2B the $T_{\rm eff}$ determined from pure hydrogen atmospheres is about 61 000 K, whereas a fit taking the metal absorption into account leads to a value about 5000 K smaller (Wolff et al. 1998).

Additionally, our values for effective temperatures above about 50 000 K can also be modified by some thousand K due to NLTE effects. This influence cannot be separated from the metal blanketing effect since the deviations from LTE depend on the amount of heavy elements in the atmosphere.

The five hottest stars in our sample have been observed with IUE with integration times between 1 800 and 10 000 sec. All measured continuum fluxes are consistent with the optically determined temperatures, but since the continuum down to 1100 Å lies well within the Rayleigh-Jeans approximation, the slope is consistent with any $T_{\rm eff} \leq 50\,000$ K.

Table 6. Upper limits on the X-ray flux of the four hottest white dwarfs of the sample from ROSAT pointings. $T_{\rm eff}$ and $\log g$ derived from different observations of the last three stars are shown individually, and separate estimates of the EUV flux have been calculated for each value. The lower limits obtained for the interstellar hydrogen density in order to account for the flux deficit is given as $N_{\rm H\,I,min}$ (Wolff, *priv. comm.*) and the measured total column density at galactic position (l, b) according to the Stark survey as $N_{\rm H\,I}(l, b)$

Object	$T_{\rm eff}$ [K]	$\log g$	B_J	$D_{\rm lum}$ [pc]	HRI cts [k s^{-1}]	$N_{\rm HI,m}$ [10^{20}/cm^2]	$N_{\rm HI}(l,b)$	l	b
HS 0615+6535	98 000	7.1	$15\overset{\rm m}{.}2$	600	< 0.6	20.0	8.4	$149\overset{\circ}{.}1$	$21\overset{\circ}{.}5$
HS 1749+7145	75 000–78 500	7.6	$15\overset{\rm m}{.}7$	400	< 0.74	13.5–14.0	4.5	$102\overset{\circ}{.}4$	$30\overset{\circ}{.}5$
HS 1827+7753	73 000–78 500	7.6–7.8	$15\overset{\rm m}{.}7$	400–340	< 0.45	14.0–16.0	4.7	$109\overset{\circ}{.}3$	$27\overset{\circ}{.}9$
HS 2246+0640	94 000–105 000	7.2–6.8	$16\overset{\rm m}{.}8$	1000–1900	< 0.78	14.0–16.0	4.5	$77\overset{\circ}{.}6$	$-44\overset{\circ}{.}9$

6. Discussion

We have presented a model atmosphere analysis for all DA white dwarfs found by the Hamburg Quasar Survey for which follow-up spectroscopy has been performed. A complete sample of all hot star candidates down to the nominal limiting magnitude of $17\overset{\rm m}{.}5$ has only been taken for one of the $5\overset{\circ}{.}5 \times 5\overset{\circ}{.}5$ fields, so that a number statistic for the different classes cannot be inferred. Star counts in this and the three other fields comprehensively observed however yield higher surface densities of DA white dwarfs than the PG survey even at magnitudes down to $16\overset{\rm m}{.}4$.

Since most of our observing runs have concentrated on very hot objects ($\gtrsim$40000 K), i.e. those showing a very blue continuum and no clear Balmer lines (visible up to about 30 000 K in the brighter DAs) on the objective prism scans, our completeness certainly increases with effective temperature; although we cannot yet specify this in a quantitative manner until we have investigated the full sample of objective prism scans (Homeier et al. in prep.), stars above 50 000 K are overrepresented.

This makes our sample complementary to the discoveries of hot stars in EUV- and soft X-ray-based surveys, since all DA white dwarfs above this temperature limit seem to contain heavy elements in their atmospheres, reducing the probability to find these stars in the EUV. On the other hand, we have found five DA white dwarfs with temperatures above 70 000 K.

The determination of stellar parameters has also shown that the selected Schmidt spectra cover at least the whole temperature range above 10 000 K for DA white dwarfs. It also confirms the possibility to distinguish between different temperature classes in the objective prism scans. Further work will determine the degree of completeness achievable at the low temperature end and near the plate limit.

Acknowledgements. We thank the Deutsche Forschungsgemeinschaft for financial support under grants He 1356/16 and Ko 738/10-1 and for several travel grants to the Calar Alto observatory. The Hamburg Quasar survey has been supported by the DFG under grants Re 353/11 and Re 353/22. Work on ROSAT observations in Kiel is supported by grants from the Deutsches Zentrum für Luft- und Raumfahrt.

We are grateful to R. Möller, T. Rauch, H. Marten, S. Haas and M. Lemke for taking spectra during the various observation runs at the DSAZ and N. Bade for providing spectra from his observations at ESO. We are much indebted to Burkhard Wolff for calculating the lower limits for the interstellar absorption for the stars observed with ROSAT.

This research has made use of the SIMBAD database, operated at CDS, Strasbourg, France, and of the Digitized Sky Survey, produced at the Space Telescope Science Institute under US Government grant NAG W-2166.

References

Barstow M.A., Fleming T.A., Diamond C.J. et al. 1993, MNRAS 264, 16
Bergeron P., Saffer, R.A., Liebert J., 1992, ApJ 394, 228
Bergeron P., Wesemael F., Beauchamp A. et al. 1994, ApJ 432, 305
Bergeron P., Wesemael F., Lamontagne R. et al. 1995, ApJ 449, 258
Böhm-Vitense E., 1958, ZAp 46, 108
Dreizler S., Werner K., 1996, A&A 314, 217
Dreizler S., Heber U., 1998, A&A, 334, 618
Dreizler S., Werner K., Jordan S., Hagen H.-J., 1994a, A&A 286, 463
Dreizler S., Heber U., Jordan S., Engels D., 1994b, Faint blue stars from the Hamburg-Schmidt Survey, in: Hot Stars in the Galactic Halo, eds. S.J. Adelman, A.R. Upgren, C.J. Adelman, CUP, p. 228
Dreizler S., Heber U., Napiwotzki R., Hagen H.-J., 1995, A&A 303, L53
Dreizler S., Werner K., Heber U., Engels D., 1996, A&A 309, 820
Eddington A.S., 1940, MNRAS 100, 354
Engels D., Cordis L., Köhler T., 1994, in: IAU Symp. 161, eds. H.T. MacGillivray et al. (Kluwer, Dordrecht), p. 317
Engels D., Hagen H.-J., Cordis L. et al. 1998, A&AS, 128, 507
Finley D.S., Koester D., Basri G., 1997, ApJ 488, 375
Giclas H.L., Burnham R., Jr., Thomas N.G., 1965, Lowell Obs. Bull. 6, 155
Giclas H.L., Burnham R., Jr., Thomas N.G., 1970, Lowell Obs. Bull. 7, 183
Giclas H.L., Burnham R., Jr., Thomas N.G., 1971, Lowell Proper Motion Survey, Northern Hemisphere (Flagstaff: Lowell Observatory)
Green, R.F., Schmidt, M., Liebert, J. 1986, ApJS 61,305
Groote D., Heber U., Jordan S. 1989, A&A 223, L1
Hagen H.-J., Groote D., Engels D., Reimers D., 1995, A&AS 111, 195
Heber U., Jordan S., Weidemann V., 1991, in White Dwarfs, NATO ASI Series, Series C, eds. G. Vauclair and E. Sion, p. 109
Heber U., Bade N., Jordan S., Voges W., 1993, A&A 267, L31
Heber U., Dreizler S., Hagen H.-J., 1996, A&A 311, L17
Heber U., Napiwotzki R., Lemke M., Edelmann H., 1997, A&A 324, L53
Iben I., Tutukov A.V., 1986, ApJ 311, 753
Jordan S., Heber U., 1993, in White Dwarfs: Advances in Observation and Theory, ed. M.A. Barstow, Kluwer, p. 47
Jordan S., Heber U., Weidemann V., 1991, in White Dwarfs, NATO ASI Series, Series C, eds. G. Vauclair and E. Sion, p. 121
Jordan S., Heber U., Engels D., Koester D., 1993, A&A 273, L27

Jordan S., Koester D., Vauclair G. et al. 1998, A&A 330, 277
Kepler S.O., Giovannini O., Kanaan A., Wood M.A., Claver C.F., 1995, Baltic Astronomy 4, 157
Koester D., Allard N.F., Vauclair G., 1994, A&A 291, L9
Koester D., Vauclair G., 1997, in: Proceedings of the tenth European Workshop on White Dwarfs, Eds J. Isern, M. Hernanz and E. Garcia-Berro, Kluwer Academic Publisher, p. 429
Lampton M., Lieu R., Schmitt J.H.M.M. et al. 1997, ApJS 108, 545
Lemke M., Heber U., Dreizler S., Napiwotzki R., Engels D., 1998, New results from the stellar component of the Hamburg Schmidt survey: A sample of sdO stars, in: The Third Conference on Faint Blue Stars, eds. A.G.D. Philip, J. Liebert, R.A. Saffer, L. Davis Press, Schenectady, NY, in press
Marsh T.R., Dhillon V.S., Duck S.R., 1995, MNRAS 275, 828
Marsh M.C., Barstow M.A., Buckley D.A. et al 1997, MNRAS 286, 369
McCook G.P., Sion E.M., 1987, ApJS 65, 603
Press W.H., Teukolsky S.A., Vetterling W.T., Flannery B.P., 1992, Numerical Recipes in FORTRAN, 2nd Edition, Cambridge University Press, Cambridge
Stark A.A., Gammie C.F., Wilson R.W. et al. 1992, ApJS 79, 77
Vennes S., Thejll P.A., Galvan R.G., Dupuis J., 1997, ApJ 480, 714
Werner K., Dreizler S., Heber U. et al. 1995, A&A 293, L75
Wolff B., Jordan S., Koester D., 1996, A&A 307, 149
Wolff B., Koester D., Dreizler S., Haas S., 1998, A&A 329, 1045
Wood M.A., 1994, in: *IAU Coll. 147: The Equation of State in Astrophysics*, eds. G. Chabrier and E. Schatzman, Cambridge University Press, Cambridge, p. 612 Lecture Notes in Physics, Springer, Berlin, p. 41
Wood M.A., 1995, in: White Dwarfs, Eds D. Koester and K. Werner, Lecture Notes in Physics, Springer, Berlin, p. 41